J Appl Electrochem (2007) 37:961–969
DOI 10.1007/s10800-007-9336-y

ORIGINAL PAPER

Electrochemical investigation of the passive behaviour of biomaterials based on Ag–Sn and Cu–Zn–Al in carbonate buffer in the absence and presence of chloride

Valéria A. Alves · Luís A. da Silva · Luís F. de F. Santos · Dane T. Cestarolli · Alexandre Rossi · Leonardo M. da Silva

Received: 11 September 2006 / Accepted: 29 April 2007 / Published online: 24 May 2007

Abstract The electrochemical behaviour of biomaterials based on Cu–Zn–Al (cubic Cu_3Zn phase) and Ag–Sn (orthorhombic Ag_3Sn and hexagonal Ag_4Sn phases) alloys was investigated in carbonate buffer solutions (pH 9.66) in the absence and presence of chloride, using different electrochemical techniques. Analyses of the open circuit potential and the potentiodynamic polarisation curves showed that the passivation domain and the corrosion parameters depend on alloy composition and chloride concentration. Chronoamperometric studies showed that passivation kinetics and corrosion of the passive film are both well described by a linear $\ln(i)$ versus $\ln(t)$ relation. The passive film formed on the Ag–Sn alloy is less susceptible to corrosion when compared to the Cu–Zn–Al system. The impedance data obtained in the passive region for the Cu–Zn–Al alloy showed that the passive layer is compact. In contrast, the impedance data obtained for the Ag–Sn alloy showed that the passive layer is formed by a compact oxide layer covered by a porous oxide gel layer. Mott–Schottky analysis showed that the passive film formed on the Cu–Zn–Al alloy behaves as a p-type semiconductor.

Keywords Corrosion · Ag–Sn · Cu–Zn–Al · Impedance spectroscopy · Passivation kinetics

V. A. Alves (✉) · L. F. de F. Santos · A. Rossi
Departamento de Farmácia, Faculdade de Ciências Biológicas e da Saúde, Universidade Federal dos Vales do Jequitinhonha e Mucuri - UFVJM, Rua da Glória, 187, Centro, Diamantina, Minas Gerais 39100-000, Brazil
e-mail: valeria@fafeid.edu.br

L. A. da Silva · D. T. Cestarolli
Departamento de Ciências Básicas, Faculdade de Ciências Agrárias, Universidade Federal dos Vales do Jequitinhonha e Mucuri - UFVJM, Rua da Glória, 187, Centro, Diamantina, Minas Gerais 39100-000, Brazil

L. M. da Silva
Departamento de Química, Faculdade de Ciências Exatas e Sociais Aplicadas, Universidade Federal dos Vales do Jequitinhonha e Mucuri - UFVJM, Rua da Glória, 187, Centro, Diamantina, Minas Gerais 39100-000, Brazil

1 Introduction

The current trend in implant science is the substitution of high-cost alloys by cheaper ones coated with protective and very stable biocompatible thin films [1–6]. The basic requirements for these films include: (i) adequate hardness and mechanical properties; (ii) considerable corrosion resistance in the oral environment and a high bonding strength with the base material [7, 8].

Besides the intrinsic mechanical properties of the biomaterial, it should be chemically inert in the oral environment, since corrosion considerably affects the biocompatibility and mechanical integrity of implants. In fact, corrosion and surface oxide film dissolution are two mechanisms that enable introduction of ions into the body which may result in biological reactions and mechanical failure of the device [9].

Corrosion of alloys in the oral environment finds its origin in the presence of several species, such as Cl^-, the hydrogen ion (H^+), sulphide compounds (S^{2-}), dissolved oxygen (O_2), and micro organisms [1–9]. For instance, chloride causes pitting corrosion, which destroys the protective passive oxide film.

Numerous surface modification treatments have been done in order to improve the corrosion behaviour, as well as the biocompatibility and mechanical properties of metallic biomaterials [2, 10]. A simple method to generate

a protective barrier on the biomaterial surface consists in manipulating the composition of the material in order to achieve conditions that favour the formation of a compact and protective passive oxide layer. The crystalline degree, average thickness and intrinsic semiconductor properties comprise the main parameters governing the protective nature of the oxide layer in the oral environment [1, 3, 4, 9].

For any biomaterial used in the human body, it is important to estimate the passivation in ''in vivo'' conditions. Therefore, appropriate modelling of the oral environment ''in vitro'' testing is necessary in order to obtain similar results to the clinical condition. However, both the chemical and physical aspects of the oral environment are complex. The use of natural saliva as the electrolyte for testing biomaterials has several limitations since saliva is unstable and contains many inorganic and organic compounds. Moreover, its composition is unique for each individual and is influenced by a number of variables, including time of day, diet and physical condition of the individual [11]. To minimise these problems, several synthetic solutions have been developed and used in corrosion tests [12]. Several aspects dealing with the electrochemical corrosion of biomaterials based on Cu-alloys in human simulated body fluids were previously discussed by Alves et al. [3].

The objective of the present work is the comparative investigation of the corrosion resistance of biomaterials based on Ag–Sn and Cu–Zn–Al alloys using different electrochemical techniques in carbonate buffer (pH 9.66) in the absence and presence of chloride ions.

2 Experimental

The alloy samples based on Ag–Sn and Cu–Zn–Al (Goldent LA, from AJE Comércio e Representações Ltda.) were prepared using the standard procedure adopted by dentists [13]. The chemical composition of the samples was determined by EDS technique with the use of a model SphinX 130 IXRF System coupled with an EVO 50 SEM instrument (ZEISS). X-ray analysis was carried out by means of a D5005 Bruker-AXS instrument using CuKα radiation (λ = 1.54056 Å).

Electrodes were prepared, in triplicate, from alloy samples in order to obtain an electrochemical geometric area of 0.95 cm^2. To avoid undesirable ohmic effects, a copper wire was connected to the back of the samples with the use of silver paint. All samples were mounted in a plastic tube and sealed with Epoxy resin. Before each experiment the working electrode was mechanically polished using 600 mesh emery paper, rinsed with pure water and dried with soft paper.

The open circuit potential (OCP) was recorded over 2 h, at 25 °C, for freshly prepared samples in different solutions. Polarisation curves, E versus $\log(i)$, were recorded sweeping the electrode potential (2.5 mV s^{-1}) from –50 mV (vs. OCP) until a potential where the anodic current density was 500 μA cm^{-2}. The anodic current located in the passive region, i_{pass}, was recorded over 1 h at fixed potentials of 0.5 and 0.1 V (vs. Ag/AgCl) for the Cu–Zn–Al and the Ag–Sn alloys, respectively, in the different solutions.

EIS measurements covered the 65 kHz–100 mHz frequency domain, resulting in 10 points per frequency decade; different d.c. potentials were applied, covering the passive region. To ensure linearity of the electrode response a small amplitude sine wave (5 mV(p/p)) was used throughout. As required by the linear system theory, validation of the EIS data was performed applying the Kramers-Kronig test [14, 15] using software acquired from the AUTOLAB® electrochemical system. For each alloy sample the impedance data were fitted using an appropriate equivalent circuit and the EQUIVCRT program of Boukamp [16].

Experiments were carried out in carbonate buffer (0.01 M Na_2CO_3 + 0.09 M $NaHCO_3$, pH 9.66) in the absence and presence of 10 and 50 mM KCl. All the electrochemical studies were carried out at 25 °C using an all-glass electrochemical cell (0.1 dm^3). A platinised platinum wire with a geometric area of 2.5 cm^2 was used as a counter electrode and all potentials were recorded against a saturated Ag/AgCl electrode. The tip of the RE was kept at ~4 mm from the sample in order to minimize the ohmic drop.

The chronoamperometric curves and the OCP measurements were recorded using a potentiostat from Microquímica, model MQPG-01. The other experiments were carried out using an AUTOLAB® (Eco Chemie, The Netherlands) electrochemical system (GPES), model PGSTAT10.

3 Results and discussion

3.1 EDS and X-ray analysis

The chemical composition of the alloys was determined by EDS. Table 1 shows the chemical composition of the alloy samples obtained from the quantitative EDS spectrum analysis.

X-ray diffraction patterns of the alloys are shown in Fig. 1. Diffractogram analysis showed that the microstructure of the Cu–Zn–Al alloy is characterized by the cubic Cu_3Zn phase, while the Ag–Sn alloy presents two phases: Ag_3Sn (orthorhombic) and Ag_4Sn (hexagonal).

Table 1 Chemical composition of the dental alloys

Alloy	Element	wt.%	Alloy	Element	wt.%
Ag–Sn	Ag	87.201	Cu–Zn–Al	Cu	73.311
				Zn	12.670
	Sn	12.799		Al	10.186
				Ni	3.832

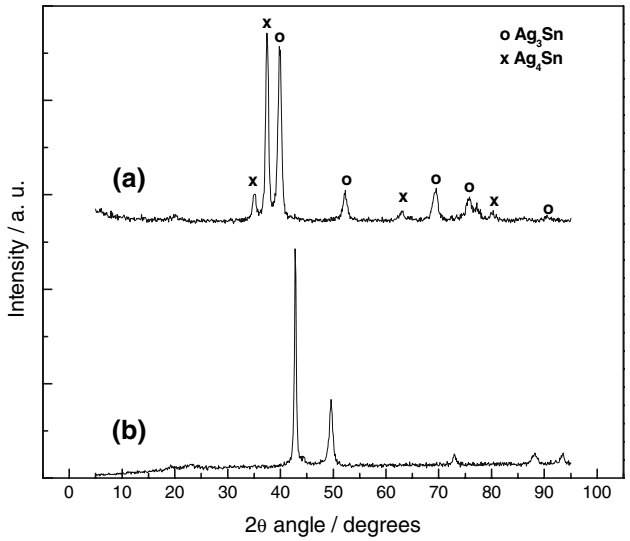

Fig. 1 X-ray diffractograms obtained for samples after surface polishment. (**a**) Ag–Sn alloy; (**b**) Cu–Zn–Al alloy

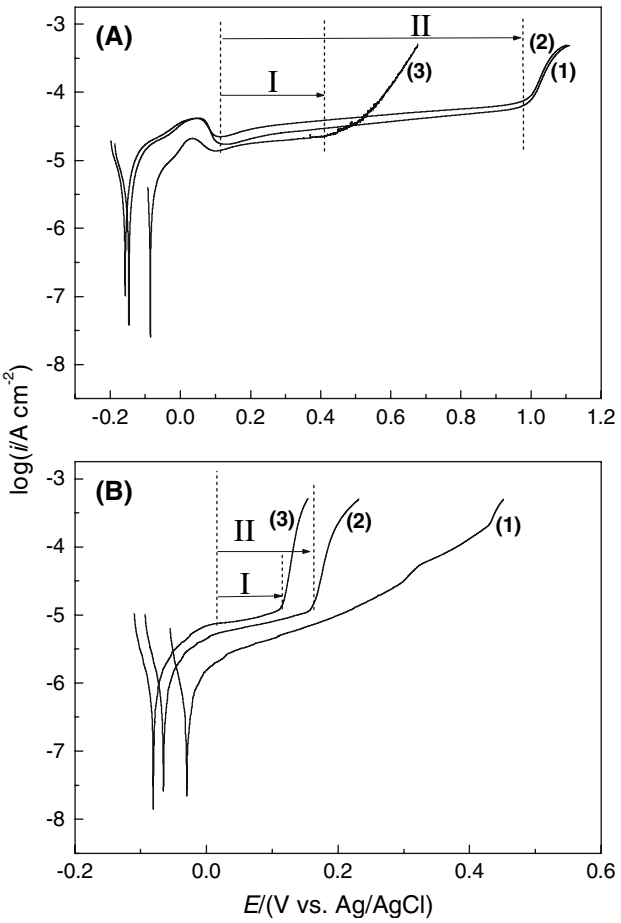

Fig. 2 Potentiodynamic polarisation curves, E versus log(i), obtained for the Cu–Zn–Al (**A**) and Ag–Sn (**B**) alloys in carbonate buffer. KCl/mM: (1) 0; (2) 10; (3) 50. T = 25 °C

3.2 Polarisation curves

Figure 2 shows potentiodynamic polarisation curves, E versus log(i), recorded under quasi-steady state conditions in carbonate buffer (pH 9.66) in the presence and absence of chloride ions, for the Cu–Zn–Al (Fig. 2A) and Ag–Sn (Fig. 2B) systems.

A comparison of Fig. 2A and B shows that the electrochemical behaviour of Cu–Zn–Al and Ag–Sn alloys is considerably different in alkaline medium. Figure 2 shows, in the case of the Cu–Zn–Al system (Fig. 2A) and in absence of chloride ions, a wide potential range (region II: ~0.1–1.0 V) where the anodic current density is very low and almost constant (passivation domain).

According to Fig. 2B, the Ag–Sn alloy has nobler (more positive) corrosion potential, E_{cor}, compared to the Cu–Zn–Al alloy. However, the passivation region for the Ag–Sn system is much narrower and even absent for the solution containing 50 mM Cl^-. These findings indicate that the passive film formed on the Ag–Sn surface is less protective at higher electrode potentials than that formed on the Cu–Zn–Al surface.

Passive films are susceptible to localized damage caused by mechanical and chemical effects. The best known chemical effect responsible for the development of localized dissolution and oxide film breakdown is caused by specific adsorption of Cl^- ions [4]. Figure 2A shows that the presence of a small chloride concentration (10 mM) is not capable of causing significant changes in the polarisation curve profile (region II), suggesting insignificant pitting corrosion. In contrast, in the presence of 50 mM Cl^- a break in the passive domain (region I) is observed, displacing the upper potential limit from ~1.0 to ~0.4 V (pitting potential, E_{pit}). This suggests that Cl^- ions at the above mentioned concentration are capable of promoting considerable breakdown of the passive film formed at the Cu–Zn–Al surface.

Figure 2B shows that for the Ag–Sn system the presence of Cl^-, despite its concentration (see regions I and II), promotes a significant change on the polarisation curve. A sudden increase in the anodic current due to pitting corrosion is observed at less noble potentials. In contrast to the Cu–Zn–Al system (Fig. 2A), the E_{pit}-value for the Ag–Sn alloy is shifted negatively with increasing Cl^- concentration.

Table 2 Corrosion parameters obtained for the Cu–Zn–Al and Ag–Sn alloys from polarisation curves

Carbonate buffer	E_{cor}/V	E_{tr}/V	E_{pit}/V	i_{cor}/μA cm^{-2}	i^{a}_{pass}/μA cm^{-2}
Alloy: Cu–Zn–Al [KCl]/mM					
0	–0.13	0.96	–	8.748	33
10	–0.12	0.97	–	6.423	44
50	–0.08	–	0.41	1.492	27
Alloy: Ag–Sn [KCl]/mM					
0	–0.03	0.29	–	0.958	5
10	–0.07	–	0.15	0.939	8
50	–0.08	–	0.11	0.411	11

[a] Measured at 0.1 and 0.5 V, for the Ag–Sn and Cu–Zn–Al alloys, respectively

The corrosion parameters for the Cu–Zn–Al and Ag–Sn alloys were determined from the potentiodynamic polarisation curves using the software available in the AUTOLAB®. Table 2 gathers the results.

The data in Table 2 show that for Cu–Zn–Al alloys the E_{cor}-values shift positively with increasing Cl^- concentration, in contrast to what is observed for Ag–Sn alloys. Although the Cu–Zn–Al system had a wider passive region (see Fig. 2A), even in the presence of Cl^- anions, this alloy had a higher passivation current, i_{pass}, and a less noble E_{cor}-value when compared to the Ag–Sn system. Table 2 also shows that the corrosion current, i_{cor}, is higher for the Cu–Zn–Al alloy. Figure 2 shows that the i_{pass} values increase with increasing Cl^- concentration for the Ag–Sn system, while in the case of the Cu–Zn–Al alloy a systematic influence of the Cl^- concentration is not observed. Based on the experimental findings presented in Table 2 and Fig. 2, it can be argued that the Ag–Sn alloy, with the exception of the solution containing 50 mM Cl^-, exhibits nobler E_{cor}-values when compared to the Cu–Zn–Al alloy. However, the more positive E_{tr} (transpassivation potential) and E_{pit} values associated with the wide passivation domain obtained for the Cu–Zn–Al alloys show that this system gives a more stable passive film.

3.3 Passive current and open circuit potential measurements for the Cu–Zn–Al and Ag–Sn alloys

The passive current at constant electrode potential is described by [17, 18]:

$$i_{pass} = \frac{A\{\exp[zKL(t)] - B\exp[-zKL(t)]\}}{\exp[zKL(t)] - 1} \quad (1)$$

where A and B are constants at a given applied potential, z is the charge of the metal ion, K is a constant (=FE/RT) related to the field strength ($\vec{E}$)and $L(t)$ is the film thickness as a function of time, t. According to Park et al. [17] Eq. 1 can be simplified for the case where the constant A has a very small value and $\exp[zKL(t)] \gg 1$, thus originating the Barbosa's model [19]:

$$\ln(i_{pass}) = \ln(k) - n \cdot \ln(t) \quad (2)$$

where i_{pass} is the passive current density, k is a constant obtained when $\ln(t) = 0$, and the slope n is the kinetic parameter representing the film growth. According to Macdonald et al. [20, 21] thicker films (>5 $\times 10^{-10}$ m) present passive current transients with $n = 1$, while for thinner films the transient is characterised by $n = 0.5$.

Figures 3 and 4 show the passive-current decay and the open circuit potential changes obtained for the Cu–Zn–Al and Ag–Sn alloys, respectively, as functions of solution composition. The OCP versus $\ln(t)$ profile is affected by the solution composition. In fact, introduction of 50 mM Cl^- leads to a considerable change in the OCP-values in the ~0–3 $\ln(t)$-domain, causing a shift to less noble OCP values. Also, one can observe that the OCP values are more positive for the Ag–Sn system.

Figures 3 and 4 show that film growth kinetics are complex giving three distinct behaviours [22–24]. Figure 3A shows passivation is characterised by a constant n value of 0.35, which reaches a null value ($n = 0$), thus indicating a stationary thickness of the passive film. Figure 3B and C show that the Cl^- concentration affects the film growth kinetics in two different ways: (i) for $[Cl^-] = 10$ mM (Fig. 3B) film thickening suffers a considerable decrease after the initial passivation stage, thus leading to a decrease in the n-value from 0.76 to 0.30. In agreement with the literature [24, 25], the kinetic profile also presents a negative n (=–0.23) due to pitting corrosion; (ii) for $[Cl^-] = 50$ mM (Fig. 3C) the film growth rate decreases ($n = 0.30$) and film corrosion by pitting is pronounced ($n = -1.7$). This behaviour is consistent with the findings presented in Fig. 2, where pitting corrosion is clearly evident.

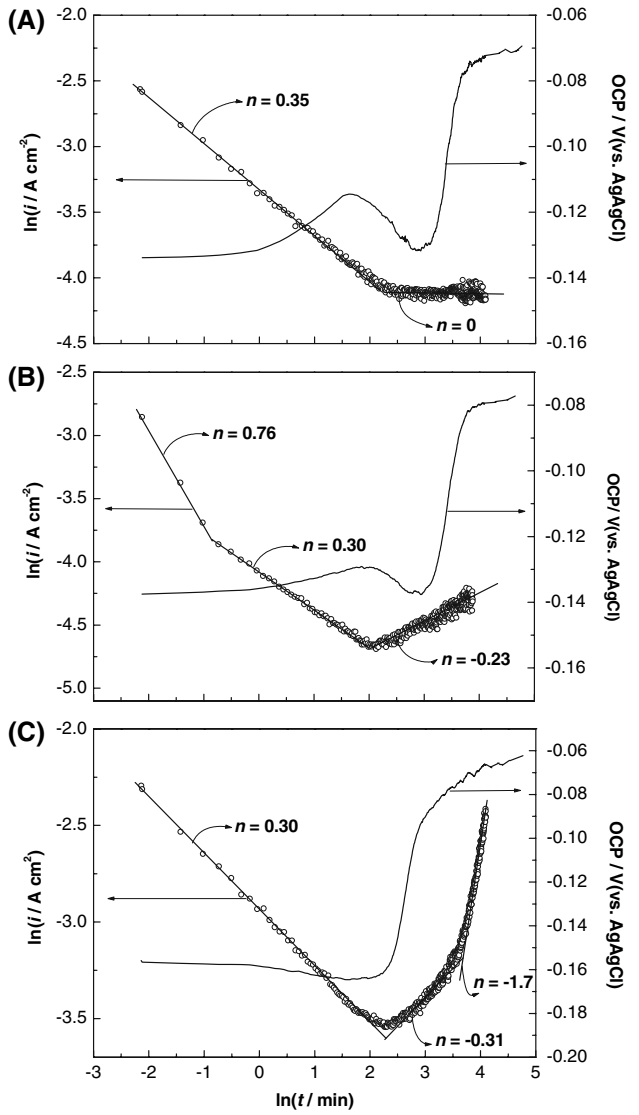

Fig. 3 Passive-current decay and open-circuit corrosion potential for the Cu–Zn–Al system in carbonate buffer. KCl/mM: (**A**) 0; (**B**) 10; (**C**) 50. E = 0.5 V. T = 25 °C

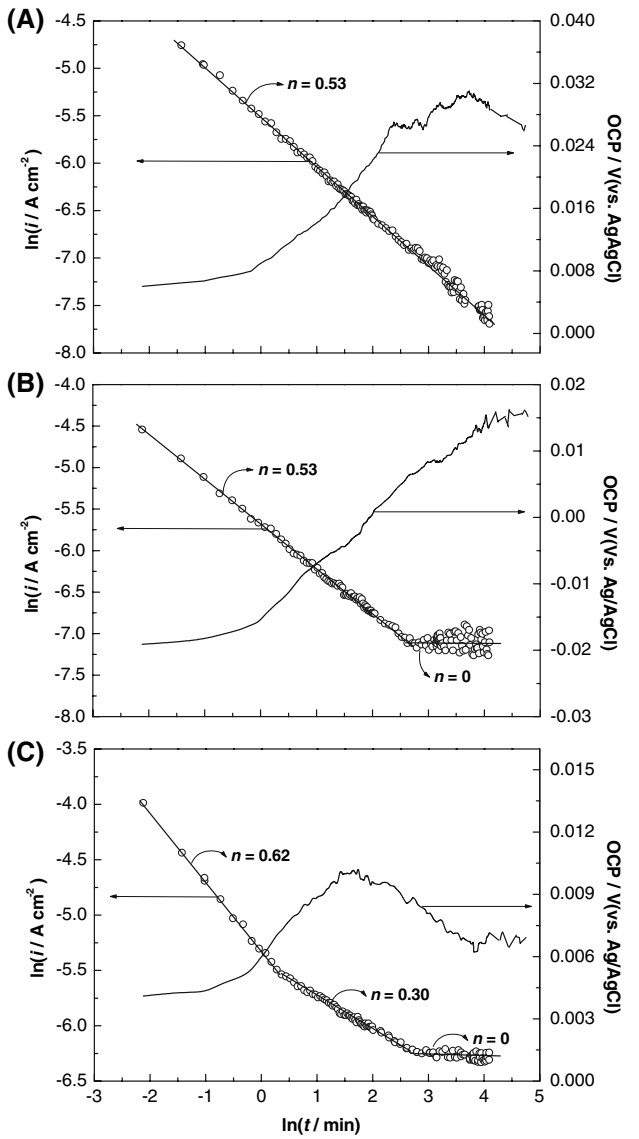

Fig. 4 Passive-current decay and open-circuit corrosion potential for the Ag–Sn system in carbonate buffer. KCl/mM: (**A**) 0; (**B**) 10; (**C**) 50. E = 0.1 V. T = 25 °C

Figure 4 shows that the Ag–Sn alloy has different passivation kinetics when compared to the Cu–Zn–Al alloy (see Fig. 3). The presence of a small amount of chloride (10 mM) does not significantly affect the passivation kinetics. Contrary to the predictions of Fig. 2, this behaviour shows that the Ag–Sn alloy has superior resistance to pitting corrosion at these potentials (0.2–0.3 V) when compared to the Cu–Zn–Al alloy. Figure 4C shows that the presence of 50 mM Cl^- considerable changes the passivation kinetics. In this case the beginning of the passivation is characterised by a higher n-value, which progressive reduces with time (0.62 → 0.30 → 0). However, as in Fig. 4B and C shows that the presence of chloride does not lead to pitting corrosion.

3.4 Electrochemical impedance spectroscopy measurements

The impedance behaviour presented by passive films can be described by equivalent circuits, EC, containing one or more time constants [1–3, 9, 26, 27]. The impedance spectra recorded in the passive region for the Ag–Sn and Cu–Zn–Al alloys are presented in Figs. 5 and 6. Figure 5 indicates the existence of one time constant, showing that the passive layer formed on the Cu–Zn–Al alloy is compact (absence of a porous oxide gel layer) [9]. The numerical analysis via Complex Nonlinear Least Squares Fitting (CNLS) of the findings obtained for the Ag–Sn alloy (see Fig. 6) showed that the passive film can be described by a

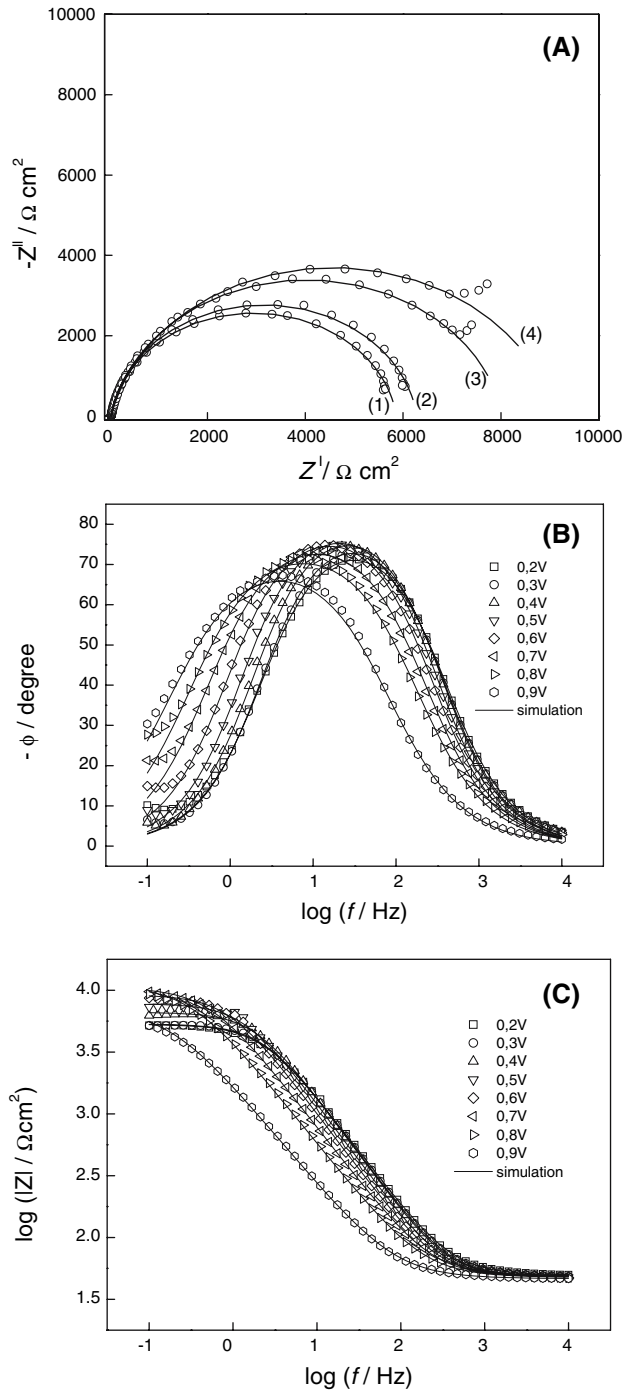

Fig. 5 Impedance spectra obtained at different potentials located in the passive region of the Cu–Zn–Al alloy, in carbonate buffer. (**A**) Complex plane, E_{dc}/V: (1) 0.2; (2) 0.3; (3) 0.4; (4) 0.5. (**B**, **C**) Bode plots

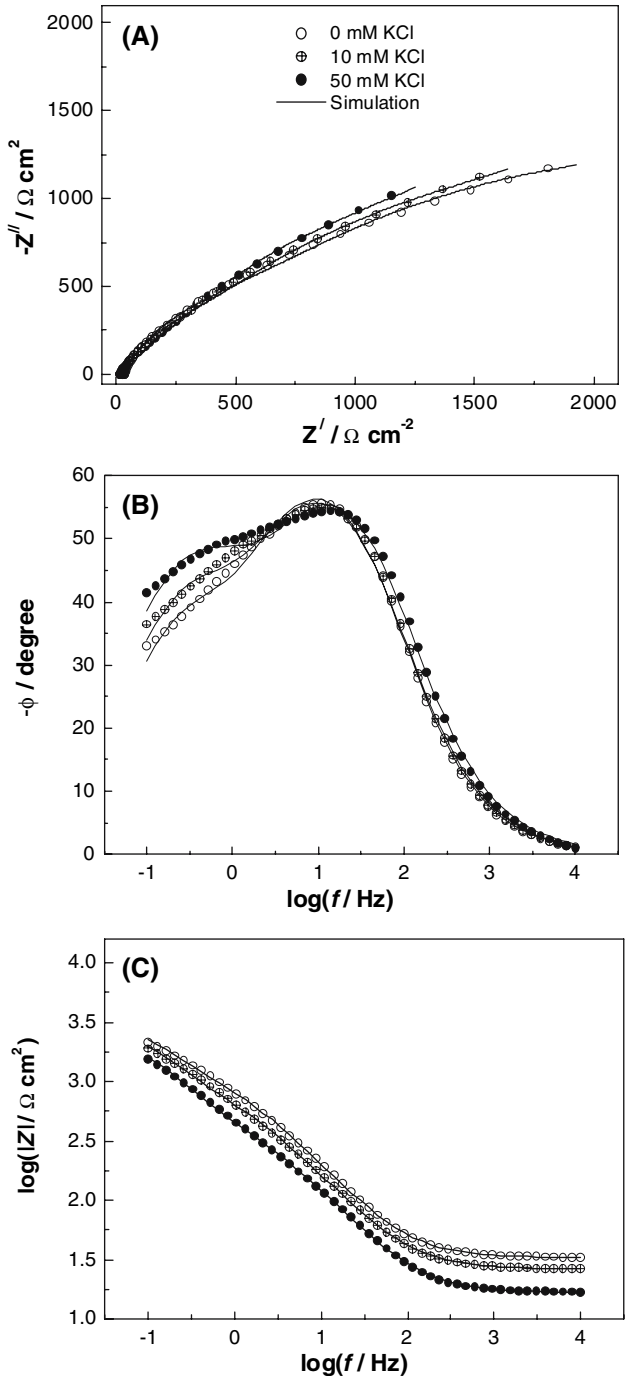

Fig. 6 Impedance spectra obtained at 0.1 V, located in the passive region of the Ag–Sn alloy, in carbonate buffer solution. (**A**) Complex plane. (**B**, **C**) Bode plots

circuit model containing two time constants. These findings are in agreement with the existence of a compact oxide layer covered by a porous oxide gel layer [9]. Figure 7 shows the equivalent circuits used for fitting the impedance spectra.

In the equivalent circuits R_Ω describes the uncompensated ohmic resistance; Q_p and Q_g are the Constant Phase Elements, CPE [28–30], used for representing the capacitive behaviour of the compact passive film and the non-compact hydrous(gel) layer, respectively; R_p and R_g are the compact passive film and gel layer resistances [2].

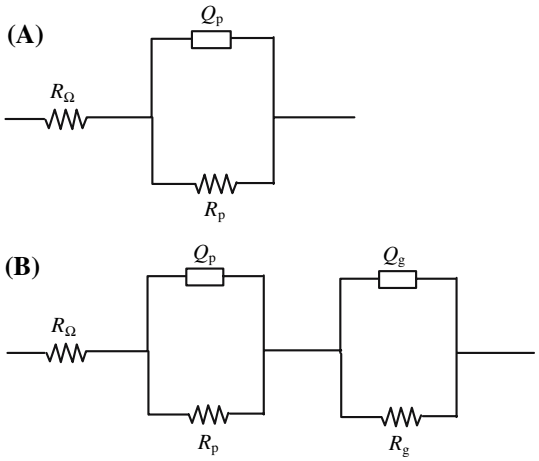

Fig. 7 Equivalent circuits used for representing the impedance response of the alloys: (**A**) Cu–Zn–Al and (**B**) Ag–Sn

The results of the numerical analysis carried out for the impedance data obtained for the Cu–Zn–Al and Ag–Sn alloys are shown in Tables 3 and 4. Table 3 shows, for all cases, that Q_p increases as the d.c. electrode potential increases. This behaviour is consistent with the semiconductor nature of the passive films (see Sect. 3.5). A comparison of the behaviour of the R_p-values as a function of the electrode potential shows a tendency of R_p to increase with the applied d.c. potential. An exception is the solution containing 50 mM Cl^-, where pitting corrosion occurs. Moreover, the high α-values support that the imaginary impedance is indeed capacitive in nature and that the passive layer is compact.

Table 3 Fitting parameters obtained from the impedance data via CNLS for the Cu–Zn–Al alloy

E/V	R_Ω/Ω cm^2	R_p/kΩ cm^2	Q_p/μF cm^{-2} s$^{(\alpha - 1)}$	α
[Cl^-] = 0 mM				
0.2	50	5.3	5.5	0.91
0.3	50	5.3	6.5	0.93
0.4	49	6.6	7.1	0.94
0.5	49	7.7	8.0	0.93
0.6	48	9.2	8.6	0.92
0.7	48	10.5	9.0	0.89
0.8	48	11.0	10.0	0.86
0.9	46	7.1	19.1	0.83
[Cl^-] = 10 mM				
0.2	35	7.4	5.1	0.90
0.3	35	6.7	5.5	0.91
0.4	36	6.3	6.1	0.91
0.5	35	6.3	6.6	0.91
0.6	34	6.8	7.1	0.88
0.7	34	7.6	7.8	0.85
0.8	33	9.4	9.8	0.81
0.9	34	1.22	33.0	0.81
[Cl^-] = 50 mM				
0.2	24	6.1	5.4	0.90
0.3	24	4.6	6.4	0.91
0.4	24	1.7	6.4	0.91

Due to the short passivation domain of the Ag–Sn alloy (see Fig. 2) the impedance spectra were obtained at two different d.c. potentials. The data of Table 4 shows that R_p are higher when compared with the R_g. These findings are consistent with the fact that the external oxide layer (gel layer) is not compact, and therefore, it allows an easier ion transport (good ionic conductance) when compared to the compact layer [2]. The values of Q_p and Q_g show that the former is considerable affected by the presence of chloride ions. This shows that the non-compact structure of the gel layer allows an intimate contact with the solution.

3.5 Semiconductor properties of the passive films

The Mott–Schottky analysis was used to investigate the semiconductor properties of passive films. Their potential dependence on the capacitance of the space charge for a p-type semiconductor, C_{SC}, is given by [28]:

$$\frac{1}{C_{SC}^2} = -\frac{2}{eN_A\varepsilon_0\varepsilon}\left(E - E_{FB} - \frac{kT}{e}\right) \quad (4)$$

where ε_0 is the vacuum permittivity, ε the dielectric constant, e the electron charge, E the applied potential, E_{FB} the flat band potential, N_A the acceptor density, and kT/e is ≅25 mV at room temperature. The acceptor density N_A can be estimated from the slope of linearly fitted Mott–Schottky plots, while the flat band potential E_{FB} can be obtained from the extrapolation of $1/C_2$ to 0.

Figure 8 shows the Mott–Schottky (M–S) plots for the passive layer formed on the Cu–Zn–Al alloy. It can be seen straight lines with a single negative slope in the M–S plots. The slope changes in the M–S plots suggest that the electronic properties (acceptor density and/or dielectric constant) are functions of the electrolyte composition. Besides, Fig. 8 shows that the flat band potential decreases as the chloride concentration increases.

4 Conclusions

The ex situ analysis showed that the microstructure of the commercial Cu–Zn–Al alloy is characterized by the cubic Cu_3Zn phase, while the commercial Ag–Sn alloy presents two phases: Ag_3Sn (orthorhombic) and Ag_4Sn (hexagonal).

The electrochemical studies carried out in carbonate buffer in the absence and presence of chloride showed that

Table 4 Fitting parameters obtained from the impedance data via CNLS for the Ag–Sn alloy

E/V	$R_\Omega/\Omega\ cm^2$	$R_p/k\Omega\ cm^2$	$Q_p/\mu F\ cm^{-2}\ s^{(\alpha-1)}$	α_p	$R_g/k\Omega\ cm^2$	$Q_g/\mu F\ cm^{-2}\ s^{(\alpha-1)}$	α_g
$[Cl^-]$ = 0 mM							
0.0	32.80	3.12	69.16	0.78	0.54	43.84	0.82
0.1	32.60	3.99	61.21	0.77	0.40	49.55	0.81
$[Cl^-]$ = 10 mM							
0.0	26.12	3.18	65.61	0.77	0.34	65.01	0.82
0.1	26.00	3.76	64.60	0.75	0.20	97.15	0.81
$[Cl^-]$ = 50 mM							
0.0	16.60	3.13	70.29	0.76	0.15	119.20	0.84
0.1	15.52	0.34	101.30	0.72	0.09	111.40	0.84

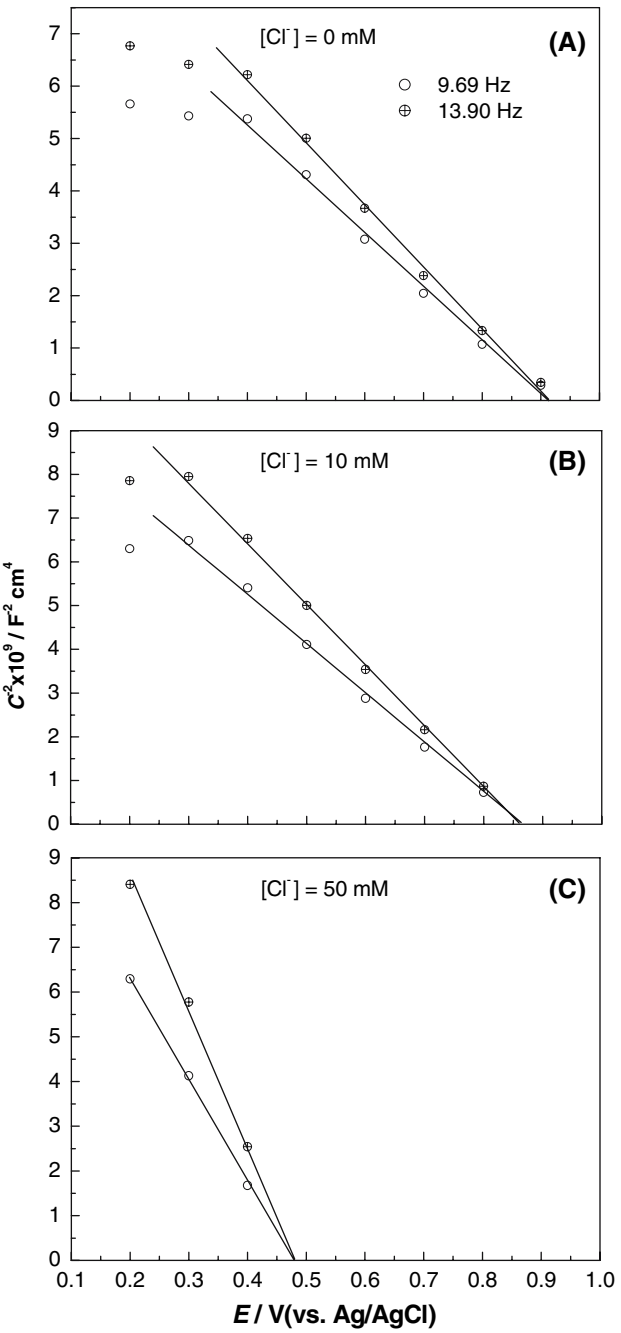

Fig. 8 Mott–Schottky plots of the Cu–Zn–Al alloy in carbonate buffer solution

the corrosion parameters and the film growth kinetics depend on the alloy composition, polarisation time and the chloride concentration. The passive film formed on the Ag–Sn alloy is less susceptible to corrosion in carbonate buffer, even in the presence of chloride, when compared to that formed on the Cu–Zn–Al system.

The impedance spectroscopy study carried out in the passive region provided information about the microstructure of the oxide films, showing that the passive layer

formed on the Cu–Zn–Al alloy is compact. In contrast, the passive layer formed on the Ag–Sn alloy contains both an inner (compact) layer and an outer (non-compact) gel layer.

Mott–Schottky analysis of the semiconductor properties of the passive film formed on the Cu–Zn–Al alloy showed that the film behaves like a p-type semiconductor. It was also found that the acceptor concentration and the flat band potential are both dependent on the chloride concentration.

Acknowledgement V. A. Alves and L. A. da Silva acknowledge financial support from FAPEMIG, FINEP and CNPq (Brazil).

References

1. Santana-Lopez A, Mirza-Rosca J, Vasilescu E, Drob P, Raducanu D, Angelescu L (2004) Mater Sci Chem Phys 86:3801
2. Shukla AK, Balasubramaniam R (2006) Corros Sci 48:1696
3. Alves VA, da Silva LA, Rossi A, Oliveira LGR, Silva TM, Vilhena MA, Santos LFF, Teixeira ELO (2006) Ciência e Tecnologia dos Materiais 18:41
4. Kwokal A, Metikos-Hukovic M, Radic N, Poljak-Guberina R, Catovic A (2003) J Mat Sci Mat Med 14:605
5. Chen B, Liang C, Fu D, Reu D (2005) Contraception 72:221
6. Ciolac S, Vasilescu E (1999) Revue Romaine de Chimie 44:431
7. Van Noort R (1987) J Mater Sci 22:3801
8. Williams DF (1987) J Mater Sci 22:3421
9. González JEG, Mirza-Rosca JC (1999) J Electroanal Chem 471:109
10. Ratner BD (1993) J Biomed Mater Res 27:837
11. Kuphasuk C, Oshida Y, Andres CJ, Hovijitra ST, Barco MT, Brown DT (2001) J Prosth Dentis 85:195
12. Gal J-Y, Fovet Y, Adib-Yadzi M (2001) Talanta 53:1103
13. Schalch MV, Adabo GL, de Souza RF, Fonseca RG, Cruz CA dos S (2004) Revista de Odontologia da UNESP 33:143
14. Kramers H (1929) Phyz Z 30:521
15. de Kronig RL (1926) J Opt Soc Ann 12:547
16. Boukamp BA (1986) Solid State Ionics 20:31
17. Park J-J, Pyun S-I, Lee S-B (2004) Electrochim Acta 49:281
18. Pyun S-I, Hong M-H (1992) Electrochim Acta 37:327
19. Barbosa M (1988) Corrosion 44:149
20. Macdonald DD (1992) J Electrochem Soc 139:3434
21. Chao CY, Lui LF, Macdonald DD (1981) J Electrochem Soc 128:1187
22. Kim J-D, Pyun S-I (1995) Electrochim Acta 40:1863
23. Raja KS, Jones DA (2006) Corros Sci 48:1623
24. Pyun S-I, Lee E-J (1995) Electrochim Acta 40:1963
25. Szklarska-Smlalowska Z (1971) Corrosion 27:223
26. Safonov VA (1993) Élektrokhimiya 29:152
27. Brown R, Alias MN, Fontana R (1993) Surf Coat Technol 62:467
28. Macdonald JR (1987) Impedance spectroscopy. John Wiley & Sons, New York
29. Brug GJ, van den Eeden ALG, Sluyters-Rehbach M, Sluyters JH (1984) J Electroanal Chem 176:275
30. Hsu CH, Mansfeld F (2001) Corrosion 57:747